Taylor & Francis
Taylor & Francis Group

Hydrological Sciences Journal

ISSN: 0262-6667 (Print) 2150-3435 (Online) Journal homepage: https://www.tandfonline.com/loi/thsj20

Testing a 1-D analytical salt intrusion model and its predictive equations in Malaysian estuaries

J.I.A. Gisen, H.H.G. Savenije, R.C. Nijzink & A.K. Abd. Wahab

To cite this article: J.I.A. Gisen, H.H.G. Savenije, R.C. Nijzink & A.K. Abd. Wahab (2015) Testing a 1-D analytical salt intrusion model and its predictive equations in Malaysian estuaries, Hydrological Sciences Journal, 60:1, 156-172, DOI: 10.1080/02626667.2014.889832

To link to this article: https://doi.org/10.1080/02626667.2014.889832 http://dx.doi.org/10.1080/02626667.2014.889832

Testing a 1-D analytical salt intrusion model and its predictive equations in Malaysian estuaries

J.I.A. Gisen[1], H.H.G. Savenije[1], R.C. Nijzink[1] and A.K. Abd. Wahab[2]

[1]*Water Resources Section, Faculty of Civil Engineering and Geosciences, Delft University of Technology, Delft, The Netherlands*
j.isabellaanakgisen@tudelft.nl
Additional address of J.I.A. Gisen is Civil Engineering and Earth Resources, Universiti Malaysia Pahang, Lebuhraya Tun Razak, 26300 Gambang, Kuantan, Malaysia

[2]*Coastal and Offshore Engineering Institute (COEI), Universiti Teknologi Malaysia Kuala Lumpur, 54100 Kuala Lumpur, Malaysia*

Received 21 June 2013; accepted 26 December 2013

Editor D. Koutsoyiannis; **Associate editor** A. Fiori

Abstract Little is known about the salt intrusion behaviour in Malaysian estuaries. Study of salt intrusion generally requires large amounts of data, especially if 2-D or 3-D numerical models are used; thus, in data-poor environments, 1-D analytical models are more appropriate. A fully analytical 1-D salt intrusion model, which is simple to implement and requires minimal data, was tested in six previously unsurveyed Malaysian estuaries (Kurau, Perak, Bernam, Selangor, Muar and Endau). The required data can be collected during a single day of observations. Site measurements were conducted during the dry season (June–August 2012 and February–March 2013) near spring tide. Data on cross-sections (by echo-sounding), water levels (by pressure loggers) and salinity (by moving boat) were collected as model input. A good fit was demonstrated between the simulated and observed salinity distribution for all six estuaries. Additionally, the two calibration parameters (the Van der Burgh coefficient and the boundary condition for the dispersion) were compared with the existing predictive equations. Since gauging stations were only present in some nested catchments in the drainage basins, the river discharge had to be up-scaled to represent the total discharge contribution of the catchments. However, the correspondence between the calibration coefficients and the predictive equations was good, particularly in view of the uncertainty in the river discharge data used. This confirms that the predictive salt intrusion model is valid for the cases studied in Malaysia. The model provides a reliable, predictive tool, which the water authority of Malaysia can use for making decisions on water abstraction or dredging.

Key words predictive salt intrusion model; salt intrusion; alluvial estuaries

Test d’un modèle analytique 1-D d’intrusion marine et de ses équations prédictives dans des estuaires de Malaisie

Résumé On connaît peu le comportement de l’intrusion marine dans les estuaires de Malaisie. Les études de l’intrusion marine nécessitent généralement de grandes quantités de données, en particulier lorsque l’on utilise des modèles numériques 2-D ou 3-D. Si les données sont peu nombreuses, des modèles analytiques 1-D sont plus appropriés. Un modèle analytique d’intrusion marine 1-D, simple à mettre en œuvre et nécessitant un minimum de données, a été testé dans six estuaires de Malaisie non étudiés auparavant (Kurau, Perak, Bernam, Selangor, Muar et Endau). Une seule journée d’observation permet de recueillir les données nécessaires à cette approche. Les mesures *in situ* ont été réalisées dans les estuaires pendant de grandes marées (juin–août 2012 et février–mars 2013). Les données sur les coupes verticales (par échosondage), les niveaux d’eau (par enregistreurs de pression) et la salinité (par bateau mobile) ont été rassemblées puis entrées dans le modèle 1-D d’intrusion marine. Cet article montre une bonne adéquation entre les distributions simulées et observées de la salinité pour les six estuaires. En outre, les deux paramètres de calage (le coefficient de Van der Burgh et la condition aux limites pour la dispersion) ont été comparés avec les équations prédictives existantes. Comme il n’existait de stations de jaugeage que dans certains sous-bassins emboîtés, le débit du fleuve a dû être extrapolé pour estimer le débit total des bassins versants. La correspondance entre les coefficients de calage et les équations prédictives est bonne, en particulier si l’on considère l’incertitude sur les données de débit de la rivière. Cela confirme que le modèle d’intrusion marine utilisé est valable pour les cas étudiés en Malaisie. Le modèle fournit un instrument prédictif fiable que les autorités en charge de l’eau en Malaisie peuvent utiliser pour prendre des décisions concernant les prélèvements d’eau ou des travaux de dragage.

Mots clefs modèle prédictif de l’intrusion marine ; intrusion marine ; estuaires alluviaux

1 INTRODUCTION

Generally, salt intrusion is a threat to people living in or near estuaries. According to statistics provided by the Malaysian Ministry of Science, Technology and Environment in 2000, over 60% of Malaysia's population (concentrated in most of the major cities) lives within or near an estuarine environment (Ong *et al*. 1991). Salt water intrusion deteriorates water supply quality and makes it unusable for daily consumption or agricultural activities. In addition, change in the intrusion may disturb the balance in the estuarine ecosystem, which may cause mangroves to grow slower or even die, reduce the variety of aquatic life, or destroy the habitat of fireflies (Van Breemen 2008). According to Van Breemen, the firefly population of Malaysian estuaries is heading towards extinction, one of the factors being salt intrusion. Changes in salinity levels may retard the growth of the berembang trees (*Sonneratia caseolaris*) that serve as the natural breeding and display grounds for fireflies. Hence, successful and effective management is required to preserve the sustainability of the resources in the estuarine ecosystem (Ibrahim *et al*. 1996).

Previous research has indicated that the salinity, the mixing mechanism in estuaries, and the salt water intrusion length (total distance salt water travels into the river system) are strongly dependent on estuary shape, tidal behaviour and the amount of freshwater discharge from the river (Ippen and Harleman 1961, Dronkers 1982, Savenije 1986, 1993, Shaha and Cho 2009). For example, water extraction and freshwater retention for aquaculture, in conjunction with sea level rise and reduced rainfall induced by climate change, will cause salinity to intrude further upstream. Several studies on salt intrusion have been carried out in South East Asia's estuaries including the Mekong estuary (Nguyen *et al*. 2008), the Chao Phya estuary (Savenije 1989), and the Red River Delta (Nguyen *et al*. 2012). Most of the earlier studies on Malaysian estuaries merely focused on how sedimentation (deposition of soil and sand into the river) affected the topography and *vice versa*. Only a few have investigated the consequence of these changes in the context of salt intrusion (Ibrahim *et al*. 1996).

There are several 1-D analytical (e.g. Kuijper and Van Rijn 2011) and 2-D and 3-D numerical models available today (e.g. MIKE 21, DELFT 3D, SWIM and HYDRUS) that can be used to analyse salt intrusion in estuaries. In the present research, the analytical salt intrusion model developed by Savenije (1986, 1993, 2005, 2012) is used because it is simple and requires a minimum amount of data. Being fully analytical, an additional advantage is that it provides a comprehensive understanding of the entire salt intrusion process. Moreover, the reliability of this salt intrusion model has been extensively tested in a wide number of estuaries around the world, including the Maputo and Incomati (Savenije 1986), the Gambia (Savenije 1988, Risley *et al*. 1993, Ervine *et al*. 2007), the Chao Phya (Savenije 1989), the Yangtze (Zhang *et al*. 2011), the Red River Delta (Nguyen *et al*. 2012) and the Mekong (Nguyen and Savenije 2006, Nguyen *et al*. 2008). Nguyen *et al*. (2008) showed that this salt intrusion model can be utilized not only in a single river channel estuary but also in multiple branch delta estuaries. Nevertheless, the model has some limitations. Savenije (2012) stated that the predictive equations of the model are still subject to improvement, and work best in natural alluvial estuaries. The predictive equations were derived on the basis of a variety of data from the literature and field measurements that were not always consistent or that had incomplete information.

The aim of this study is to test the effectiveness of the existing salt intrusion model at six previously unsurveyed estuaries in Malaysia and to discover if any modification is required. To successfully perform the analysis using the analytical model, real time data is required. Hence, on-site data collections of the topography and salinity concentration in the estuaries were carried out during the dry season near spring tide in the period June–August 2012 and February–March 2013. Shape (geometry) and salinity analyses were performed on each of the estuaries. The calibrated dimensionless parameters were subsequently compared to the predictive equations, to test their applicability in Malaysian estuaries. Finally, adjustments were made to cater for the ungauged parts of the catchments draining to the estuaries.

2 STUDY AREAS

In this study, six previously unsurveyed estuaries in Malaysia were selected: the Kurau, the Perak, the Bernam, the Selangor, the Muar and the Endau. Moreover, the runoff of the catchments draining to these estuaries is insufficiently known. Only some nested catchments within the drainage basins are gauged, but large parts are not. All these estuaries except the Endau are located on the west coast of

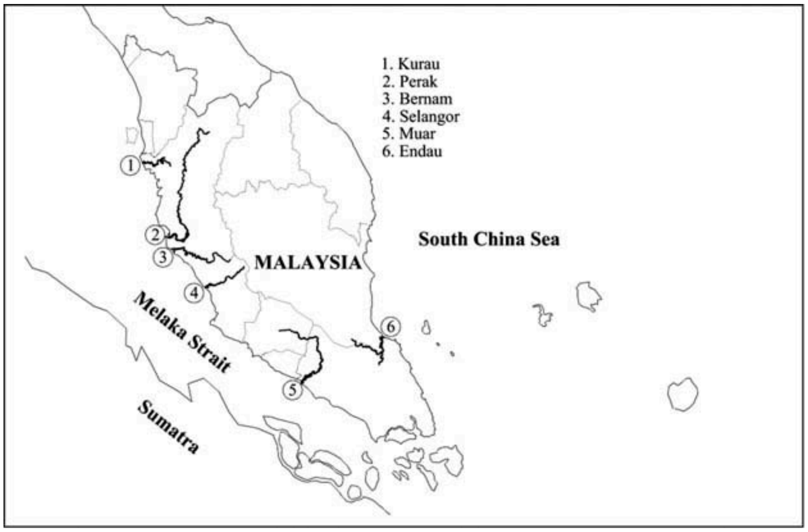

Fig. 1 Overview of the river estuaries studied (not to scale): rivers are highlighted with darker lines.

Peninsular Malaysia, and along the Malacca Strait where the mouth faces the east coast of Sumatra, Indonesia (Fig. 1). The Endau estuary is located on the east coast of the peninsula facing the open South China Sea. The rivers draining to these estuaries are between 90 and 400 km long, with catchment areas of 2000–14 000 km^2 as tabulated in Table 1.

Most of the studied estuaries are natural with little human interference except for the Muar. The Kurau is surrounded by paddy fields while agriculture is the main economic activity. Medium-scale commercial fishing and aquaculture farming can also be found in this estuary. The Perak and Bernam estuaries are situated next to each other separated by a small town named Bagan Datoh. Both catchments are covered with oil palm plantations which provide the main economic activity. In the Bernam estuary, the wide river mouth provides a good environment for medium-scale commercial fishing. The Selangor estuary is a natural park which is famous for watching fireflies (Van Breemen 2008). Moreover, it is also well-known for its large-scale commercial fishing activity. As for the Muar estuary, the densely populated Muar town is situated on the banks of the river mouth. This estuary is relatively deep due to dredging and sand mining. Some areas surrounding the Endau estuary are covered by paddy field, while the majority has remained untouched and covered with forest reserves. The famous Endau-Rompin National Park is located about 100 km upstream from the river mouth. The Endau River serves as the border between Pahang and Johore states. Figure 2(a)–(f) presents aerial views of all the estuaries. There are three freshwater inlets situated at 3, 11 and 15 km along the Selangor River estuary Fig. 2(d). These inlets drain water into the river during heavy rain to prevent the land from flooding.

Table 1 General information of the surveyed estuaries (source: EPU 1982).

No.	Estuary	Coastline	State	River length (km)	Catchment area (km^2)
1	Kurau	west	Perak	100	3 255
2	Perak	west	Perak	400	14 000
3	Bernam	west	Selangor	200	3 335
4	Selangor	west	Selangor	120	1 960
5	Muar	west	Johore	230	6 160
6	Endau	east	Johore	95	4 740

All estuaries on the west coast experience a dominant semi-diurnal tide with a 12.4-hour tidal cycle. The pattern of the tidal oscillation remains the same throughout the year. The Endau estuary, situated on the east coast, has a mixed-diurnal and semi-diurnal tide. The difference between the two tidal behaviours can be seen in Fig. 3(a) and (b). At spring tide, the tidal amplitude of the Kurau, Perak, Bernam, Selangor, Muar and Endau estuaries ranges from 2 to 4 m, while at neap tide it varies from 0.2 to 1 m. Every year from June to September, the west coast estuaries are slightly affected by the Southwest Monsoon from the Indian Ocean. The impact is small because the coastline is protected by Sumatra Island but, as a result, the salinity in the Malacca Strait is lower as the freshwater discharge from the rivers

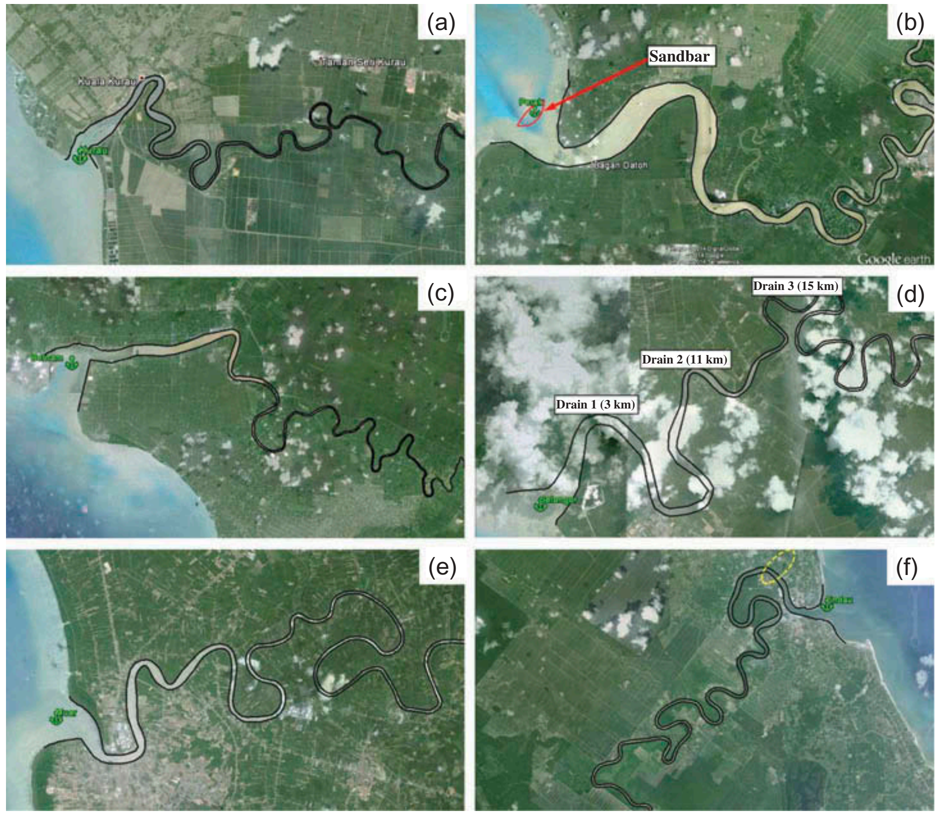

Fig. 2 Aerial views of the estuaries from Google Earth (not to scale): (a) Kurau estuary; (b) Perak estuary with sand bar; (c) Bernam estuary; (d) Selangor estuary with three drainage sluices; (e) Muar estuary; and (f) Endau estuary with one estuary tributary marked by a dotted line.

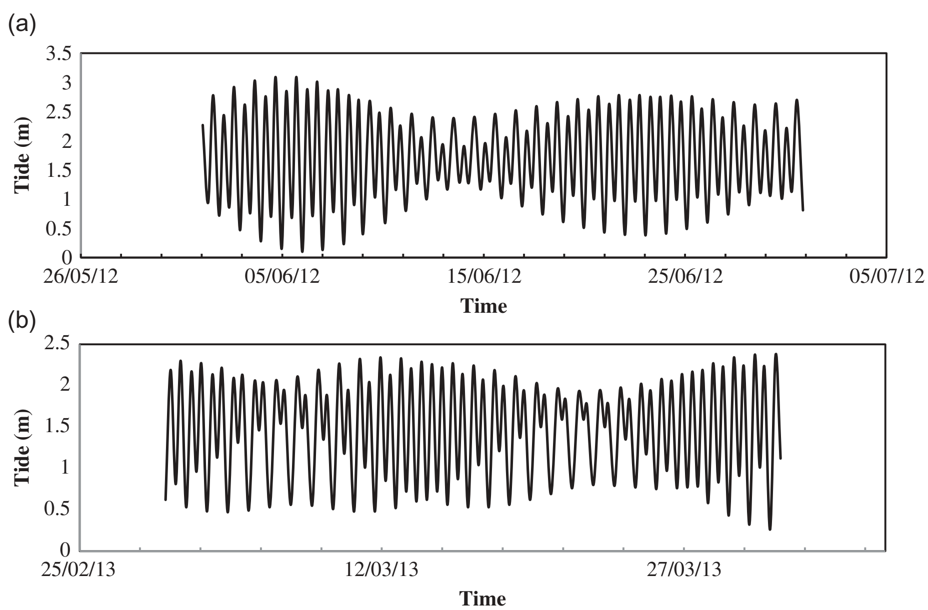

Fig. 3 (a) Tidal oscillations in Bagan Datoh station (used for Bernam estuary) showing a dominant semi-diurnal tide; (b) tidal oscillations in Tanjong Sedili Kecil station (used for Endau estuary) showing a mixed-tide tidal.

Table 2 Tidal range and average discharge information of the surveyed estuaries.

Estuary	Tidal range (m) Spring	Neap	Average discharge (m^3/s) Wet	Dry
Kurau	2.5	0.5	20	15
Perak	3	0.6	280	190
Bernam	3	0.6	90	30
Selangor	4	1.0	100	30
Muar	2	0.2	170	30
Endau	2	0.2	50	20

draining towards the straits has diluted the salt water. From February to March, the west coast estuaries are not affected by the Northeast Monsoon, but the Endau estuary on the east coast is considerably affected.

Besides the tide, salt intrusion mainly depends on the amount of freshwater draining into the estuary. Generally, the dry season in Malaysia lasts from May to August, and the wet season is from September to April (Van Breemen 2008). Nevertheless, on the west coast of the Peninsula, there is a short dry period which takes place in February. An accurate estimate of the freshwater discharge in the tidal region is difficult to obtain. Large parts of the catchments are ungauged and most of the streamflow stations are located about 100 km or further from the estuary mouth. Based on the nearest streamflow stations available, the monthly averaged discharges for each of the river estuaries during the dry and wet season are displayed in Table 2.

All estuaries have a clear trumpet shape. The wide mouths of the estuaries are wave dominated, whereas the gradually converging estuary channels emerge from the balance between tide and river discharge. Regarding the salinity mixing mechanism, Ibrahim *et al*. (1996) mentioned that estuaries on the central west coast of Peninsular Malaysia are of the partially-mixed type. However, site observations showed that four of the estuaries (Kurau, Bernam, Muar and Endau) were well-mixed, while the other two estuaries (Selangor and Perak) were partially-mixed (meaning that there is a gradual increase of salinity over the depth). The partially-mixed form results from a relatively large river discharge compared to tidal flows.

3 BACKGROUND THEORIES

Savenije's salt intrusion model (1986, 2005, 2012) involves two components: the shape analysis and the longitudinal salinity distribution of an estuary. In shape analysis, the geometry of an alluvial estuary can be presented by exponential functions. According to Nguyen *et al*. (2008), Zhang *et al*. (2011) and Nguyen *et al*. (2012), this shape model can also be applied in multi-channel and multi-reach estuaries. Estuaries that do not experience strong ocean waves near the mouth can generally be described by a single reach with only one convergence length, whereas those that experience strong waves near the mouth generally have two reaches with two convergence lengths; a short reach close to the sea with a short convergence length and a long one upstream with a longer convergence length. The equations for the shape analysis are written as:

$$A = A_0 e^{-\frac{x}{a_1}} \quad \text{for } 0 < x \le x_1 \tag{1}$$

$$A = A_1 e^{-\frac{(x-x_1)}{a2}} \quad \text{for } x > x_1 \tag{2}$$

$$B = B_0 e^{-\frac{x}{b_1}} \quad \text{for } 0 < x \le x_1 \tag{3}$$

$$B = B_1 e^{-\frac{(x-x_1)}{b_2}} \quad \text{for } x > x_1 \tag{4}$$

$$h = h_0 e^{\frac{x(a_1-b_1)}{a_1 b_1}} \quad \text{for } 0 < x \le x_1 \tag{5}$$

$$h = h_1 e^{\frac{(x-x_1)(a_2-b_2)}{a_2 b_2}} \quad \text{for } x > x_1 \tag{6}$$

where A [L^2], B [L] and h [L] represent the cross-sectional area, width and average depth at distance x [L]; A_0 [L^2], B_0 [L] and h_0 [L] are the cross-sectional area, width and average depth at the estuary mouth; and a [L] and b [L] are the cross-sectional and width convergence length. The longitudinal distance, x_1 [L] is the inflection point where the wave dominated region ends and where there is a change in the convergence length. At this point, the cross-sectional area, width and average depth become A_1 [L], B_1 [L] and h_1 [L]. Also at this point, the convergence lengths switch from a_1 [L] to a_2 [L] and from b_1 [L] to b_2 [L]. The average depth is obtained by dividing the cross-sectional area by the width. Savenije (2005) mentioned that in ideal alluvial estuaries, the convergence lengths a and b are approximately equal (near constant depth).

Integrating the shape analysis (see equations (1)–(6)) with the salt balance equation, using the Van der Burgh (1972) equation for longitudinal dispersion leads to the following that describe the salt intrusion. The longitudinal variation of salinity along the estuary (from the mouth to where the water becomes totally fresh) for a steady state condition (Savenije 2005, 2012) is given by:

$$\frac{S - S_f}{S_0 - S_f} = \left(\frac{D}{D_0}\right)^{\frac{1}{K}} \text{ for } 0 < x \leq x_1 \tag{7}$$

$$\frac{S - S_f}{S_1 - S_f} = \left(\frac{D}{D_1}\right)^{\frac{1}{K}} \text{ for } x > x_1 \tag{8}$$

The parameters S [ML^{-3}] and D [L^2 T^{-1}] are the salinity and dispersion as a function of the distance, while S_0 [ML^{-3}] and D_0 [L^2 T^{-1}] represent the salinity and dispersion at the estuary mouth. At the inflection point, the dispersion and salinity are represented by D_1 [L^2 T^{-1}] and S_1 [ML^{-3}]. The freshwater salinity is expressed by S_f [ML^{-3}], which is normally close to 0. Similar to the geometry equations, the salinity and dispersion (equations (7)–(14)) are split into two sections—the mouth and upper region:

$$\frac{D}{D_0} = 1 - \beta_0 \left(\exp\left(\tfrac{x}{a_1}\right) - 1\right) \quad \text{for } 0 < x \leq x_1 \tag{9}$$

and

$$\frac{D}{D_1} = 1 - \beta_1 \left(\exp\left(\tfrac{x - x_1}{a_2}\right) - 1\right) \quad \text{for } x > x_1, \tag{10}$$

with:

$$\beta_0 = \frac{K a_1 Q_f}{D_0 A_0} = \frac{K a_1}{\alpha_0 A_0} \text{ for } 0 < x \leq x_1 \tag{11}$$

$$\beta_1 = \frac{K a_2 Q_f}{D_1 A_1} = \frac{K a_2}{\alpha_1 A_1} \text{ for } x > x_1 \tag{12}$$

and:

$$\alpha_0 = \frac{D_0}{Q_f} \text{ for } 0 < x \leq x_1 \tag{13}$$

$$\alpha_1 = \frac{D_1}{Q_f} \text{ for } x > x_1 \tag{14}$$

where Q_f [L^3 T^{-1}] is the freshwater discharge and K is the Van der Burgh coefficient, which ranges between 0 and 1 (Savenije 2005); D_0 [L^2 T^{-1}] and D_1 [L^2 T^{-1}] represent the dispersion coefficient; and β_0 [-] and β_1 [-] are the dispersion reduction rate at the estuary mouth and at the inflection point, respectively. Due to the difficulty of obtaining discharge and dispersion estimates, they are conveniently combined in the mixing number, α_0 [L^{-1}] and α_1 [L^{-1}], which facilitates calibration. The final objective in salt intrusion analysis is to obtain the furthest distance the salt water penetrates into the estuary system. Following from equation (10), the salt intrusion length L [L] can be computed for $D = 0$:

$$L^{\text{HWS}} = x_1 + a_2 \ln\left(\frac{1}{\beta_1} + 1\right) \tag{15}$$

Savenije (2005, 2012) proposed calibration of the salinity curve on the high water slack (HWS) salinity observations, which is the best condition for observing the entire intrusion curve. It was demonstrated that the shape of the curve at the low water slack (LWS) and tidal average (TA) condition is the same, the difference being the horizontal translation of the curves over the tidal excursion E and $E/2$, respectively. This shift also applies to the dispersion, as explained in equations (16)–(23) for a single reach estuary (Savenije 1989):

$$\frac{S^{\text{HWS}} - S_f}{S_0^{\text{HWS}} - S_f} = \left(\frac{D^{\text{HWS}}}{D_0^{\text{HWS}}}\right)^{\frac{1}{K}} \tag{16}$$

$$D^{\text{HWS}} = D_0^{\text{HWS}} - \frac{K a Q_f}{A_0}\left[\mathrm{e}^{\left(\frac{x}{a}\right)} - 1\right] \tag{17}$$

The relation between the salinity and dispersion at TA and HWS are as follows:

$$S_0^{\text{TA}} = S^{\text{HWS}}(E/2) \tag{18}$$

$$S^{\text{TA}}(E/2) = S^{\text{HWS}}(E) \tag{19}$$

$$\frac{S^{\text{HWS}}(E)}{S^{\text{HWS}}(E/2)} = \frac{S^{\text{TA}}(E/2)}{S_0^{\text{TA}}} \ldots$$
$$\ldots = \left[1 - \frac{KaQ}{A_0 D^{\text{HWS}}(E/2))} \frac{\mathrm{e}^{\left(\frac{E}{2a}\right)} - 1}{\mathrm{e}^{\left(-\frac{E}{2a}\right)}}\right]^{\frac{1}{K}} \tag{20}$$

$$D_0^{\mathrm{TA}} = \left\{ \begin{array}{l} D_0^{\mathrm{HWS}} - \ldots \\ \ldots \frac{KaQ_f}{A_0}\left[\mathrm{e}^{\left(\frac{E}{2a}\right)} - 1 \right] \end{array} \right\} \mathrm{e}^{\left(-\frac{E}{2a}\right)} \tag{21}$$

For the LWS situation, the salinity and dispersion is shifted in a total length of the tidal excursion as shown below:

$$S_0^{\mathrm{LWS}} = S^{\mathrm{HWS}}(E) \tag{22}$$

$$D_0^{\mathrm{LWS}} = D^{\mathrm{HWS}}(E)\mathrm{e}^{\left(-\frac{E}{a}\right)} \tag{23}$$

Since the D_0 and K are two calibration parameters in the salt intrusion model, the model can only be predictive if separate equations for K and D_0 are available. Predictive equations were presented by Savenije (1993), and later improved by Nguyen and Savenije (2006) with larger datasets. The empirical predictive equations are expressed as:

$$\frac{D_0^{\mathrm{HWS}}}{\upsilon E} = 1400 \frac{\bar{h}}{a} \sqrt{N_R} \tag{24}$$

$$K = 0.2 \times 10^{-3} \left(\frac{E}{H}\right)^{0.65} \left(\frac{E}{C^2}\right)^{0.39} \ldots \ldots (1 - \delta b)^{-2.0} \left(\frac{b}{a}\right)^{0.85} \left(\frac{Ea}{A_0}\right)^{0.14} \tag{25}$$

where $D_0{}^{\mathrm{HWS}}$ [-] is the dispersion coefficient at estuary mouth during HWS, $\bar{h}$ [L] is the average depth, H [L] is the tidal range, C [$L^{0.5}$ T^{-1}] is the Chezy roughness, and δ [L^{-1}] is the damping rate, with:

$$N_{\mathrm{R}} = \frac{\Delta\rho}{\rho} \frac{ghQ_f T}{A_0 E_0 \upsilon_0^2} \tag{26}$$

and

$$E_0 = \frac{\upsilon_0 T}{\pi} \tag{27}$$

The estuarine Richardson number N_{R} is defined in equation (26), where ρ [ML^{-3}] is the water density, $\Delta\rho$ is the density difference over the intrusion length, g [L S^{-2}] is the gravitational force, T [T] is the tidal period, and υ_0 and E_0 are the velocity amplitude and tidal excursion, respectively, at the mouth.

In this paper, we have tested the applicability of these predictive equations in a range of very different previously unsurveyed estuaries, whose characteristics are presented in the next section. In order to utilize the predictive equations for the dispersion, the freshwater discharge into the estuary on the day of measurement has to be known. However, it is difficult to determine this discharge in the tidal region accurately. This issue is discussed in Section 6.

4 DATA AND OBSERVATIONS

The data required for applying the salt intrusion model were collected on-site or obtained from local authorities in Malaysia. Field measurements were conducted during the dry season at Kurau, Perak, Bernam, Selangor, Muar and Endau estuaries, with the assistance of the Institute of Coastal and Offshore Engineering, Universiti Teknologi Malaysia (UTM). The measurements were carried out at spring tide from February to March and mid-June to early August. The data measured during the field work were: the salinity along the estuary; the variation of the water level; and the cross-sectional areas along the salt intrusion length.

Before salinity and cross-section measurements were carried out, three or four CTD and TD-Divers (pressure recorders used to measure water level) were first installed along the estuaries: a CTD-Diver has corrosion-proof housing and is able to record conductivity which makes it suitable for installation at the mouth. Divers were installed during low water to make sure they were submerged in the water even during lowest tide. Polyvinyl chloride (PVC) pipes with holes were used to hold the divers in place, and the pipes were tied to the column of a jetty. The divers were previously set and initiated to record water level data for every minute.

Next, salinity measurements were carried out during high water slack (HWS—when the flow changes direction after high water) and low water slack (LWS—when the flow changes direction after low water) by a moving boat technique, moving with the speed of the tidal wave at HWS and LWS (see Savenije 2005, 2012). The maximum and minimum salinity curves at HWS and LWS were thus observed, representing the envelopes of the salinity variation during a tidal cycle. A conductivity meter attached to a 10 m cable was used to measure the salinity at every meter over the vertical. The measurements started from the mouth moving upstream, keeping pace with the tidal wave until the salinity level reached 0.1 ppt.

The observed salinities obtained at HWS for all six estuaries are presented in Figs. 4(a)–(f). From these figures, it can be summarized that the mixing mechanism in the studied areas consists of two types: well-mixed and partially-mixed. The vertical salinity distribution patterns along the reach indicate that the estuaries that are located on the northern-west and east coast have a partially mixed behaviour, while those on the centre-west coast are well-mixed. For the Selangor estuary, the deviating reading at 12 km from the mouth is caused by the discharge of a drainage outlet due to heavy local rain. The findings on the vertical salinity distribution in these surveys show disagreement with the statement by Ibrahim *et al.* (1996), who claimed that the estuaries on the centre-west coast of Peninsular Malaysia are partially-mixed type (of course this depends on the river discharge at the time of observation).

Cross-sectional profiles of the estuaries were also surveyed by boat with a hand-held sonar system and GPS, after the divers were installed. The cross-sectional areas were determined in relation to the observed mean tidal level and not in relation to some surveying datum or temporary benchmark, which were not available. At least 20 cross-sections were recorded for each estuary, from the mouth up to a few kilometres beyond the final stop of the salinity measurements. The date and times of measurements were noted precisely in order to correct the observed depth in accordance with the water level recorded by the divers. The results of the cross-sectional observations are presented in Fig. 5 and Table 3, demonstrating that the geometry consists of two reaches following exponential functions.

Finally, information is required on river discharge. Unfortunately, it is difficult to measure the discharge just outside the tidal region as it is time and energy consuming. As an alternative, discharge data were requested and obtained from the Department of Irrigation and Drainage, Malaysia (DID)—the

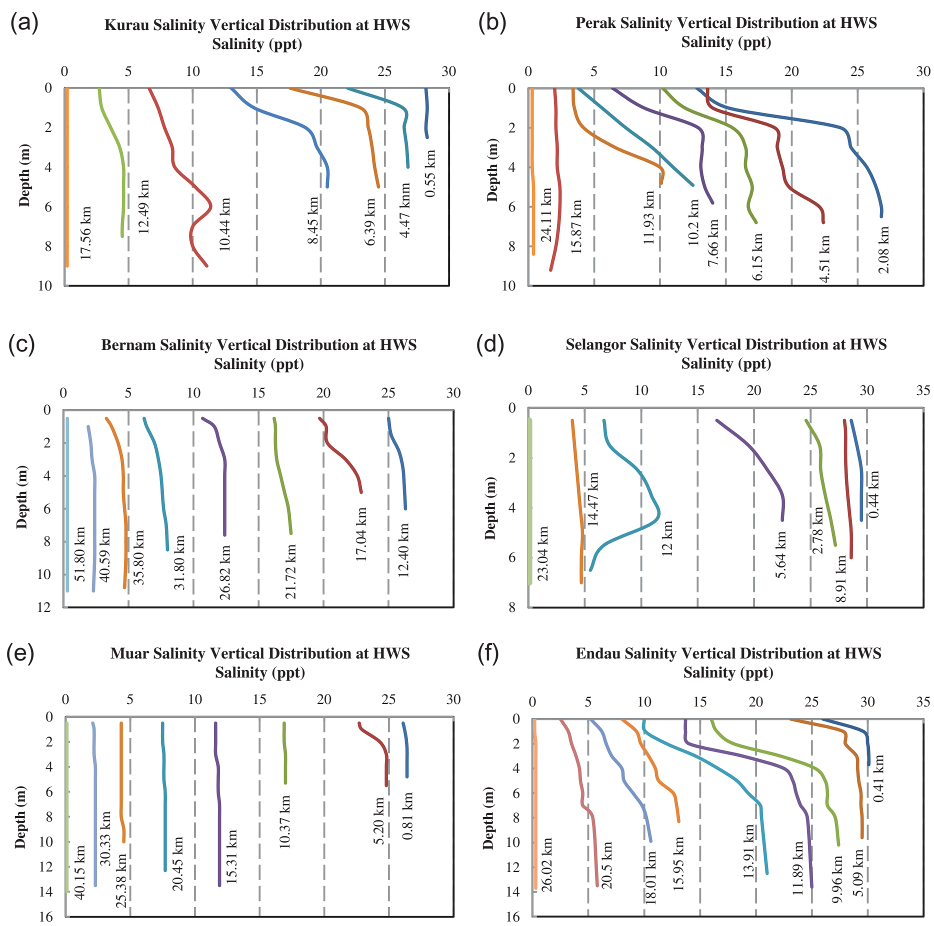

Fig. 4 Measured vertical salinity distribution of the estuaries: (a) Kurau (survey date 28 February 2013); (b) Perak (14 March 2013); (c) Bernam (21 June 2012); (d) Selangor (24 July 2012); (e) Muar (3 August 2012); and (f) Endau (28 March 2013), showing the salinity distribution at HWS (High Water Slack).

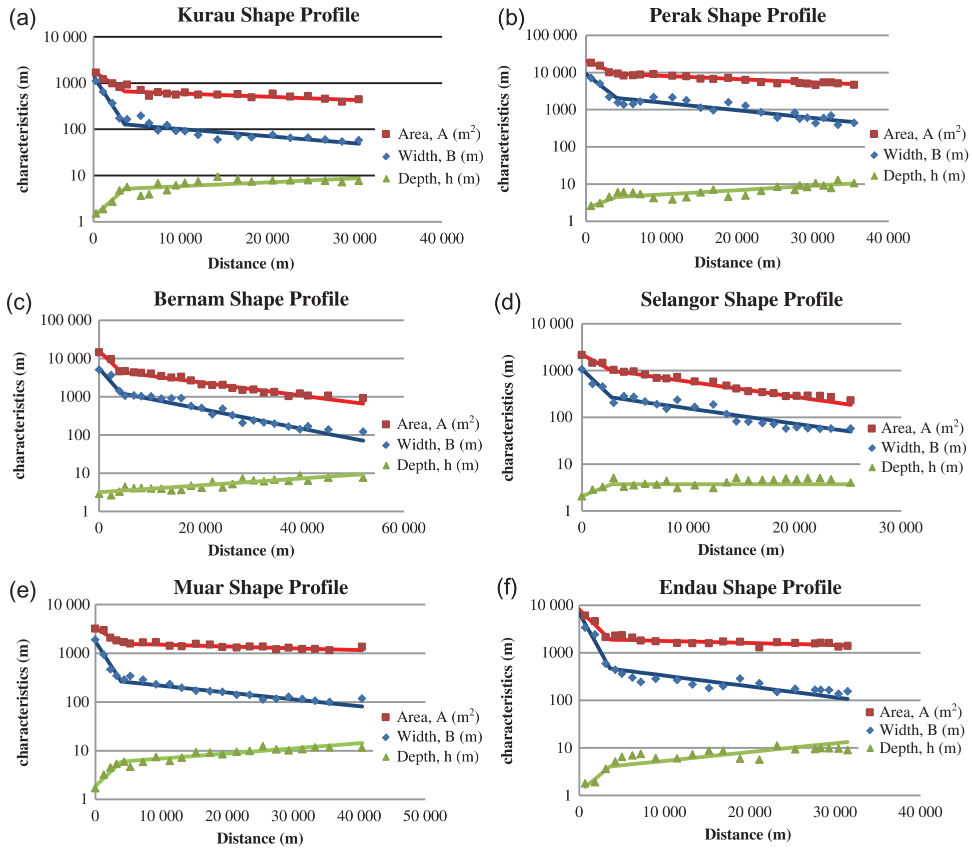

Fig. 5 Shape of the estuaries at tidal average: (a) Kurau; (b) Perak; (c) Bernam; (d) Selangor; (e) Muar; and (f) Endau, displaying the cross-sectional area (m^2), width (m) and depth (m).

Table 3 The geometry and tidal characteristics of the estuaries showing the cross-sectional area A, channel width B, cross-sectional area convergence length a, width convergence length b, estuary's average depth $\bar{h}$, and tidal range H. (For A and B, the subscripts 0 and 1 refer to the location at the mouth and inflection point, whereas for a and b, these locations are represented by subscripts 1 and 2, respectively.)

Estuary	A_0 (m^2)	A_1 (m^2)	B_0 (m)	B_1 (m)	a_1 (m)	a_2 (m)	b_1 (m)	b_2 (m)	$\bar{h}_{obs}$ (m)	H (m)
Kurau	1 800	660	1 400	130	3 600	62 000	1 500	28 000	5.9	2.0
Perak	20 500	9 200	9 100	2 070	5 000	49 000	2 700	21 000	6.1	2.8
Bernam	15 800	4 500	5 600	1 240	3 400	25 000	2 900	16 700	5.2	2.9
Selangor	2 200	1 000	1 060	270	3 500	13 400	2 000	13 400	3.6	4.0
Muar	3 300	1 600	1 750	260	5 300	118 000	2 100	30 800	7.9	2.1
Endau	8 000	1 900	6 700	460	2 500	100 000	1 350	19 000	7.2	1.9

authority in charge of the river networks in Malaysia. However, drainage basins of the estuaries are only partially gauged, the effect of which will be dealt with in Section 6.

5 RESULTS AND ANALYSES

Essentially, the topography and salinity analyses carried out in this study are based on the tidal average (TA) condition. However, the exisiting predictive equation for the dispersion D_0 was developed for the HWS condition. To compare and verify the calibrated D_0 with the predicted value, we calibrated for both the HWS and TA situations. All the results from the calibration were then applied in equations (7)–(8) to compute the longitudinal salinity distribution in an estuaryfor the three tidal conditions: high water slack

(HWS), tidal average (TA) and low water slack (LWS).

5.1 Geometry of the estuaries

The geometry analyses were performed by utilizing equations (1)–(6) and the results prove that the shapes of the estuaries indeed follow an exponential function. All the estuaries studied appear to consist of two width and cross-sectional convergence lengths: a_1, a_2, b_1 and b_2. Figure 5 indicates that the convergence length is shorter near the estuary mouth (which is a wave dominated region) compared to the section after the inflection point, which is tide dominated. All the estuaries except the Selangor present different values of cross-sectional and width convergence length, which indicate a gradual depth increase in the upstream direction; Table 3 summarizes the results from the analyses. The Selangor plot showed the convergence lengths a and b to be almost equal, with an almost constant depth. The Muar River estuary is the deepest among the five, which may be partly caused by dredging; sand barges carry tonnes of mined sand to the sea.

5.2 Salinity analysis

On the basis of the geometry data, the longitudinal salinity distributions along the river estuaries were calculated using equations (7)–(14). All analyses were performed based on both HWS and TA conditions, on the basis of which the dispersion for both situations is calculated using equations (17) and (21). The Van der Burgh coefficient K and dispersion D_0 were calibrated so as to obtain the best fit between the simulated salinity variations and the observed salinity data. Considering that the velocity amplitude was not measured during the survey, the tidal excursion E was also obtained from calibration and is considered constant along the channel. Due to the difficulty in measuring discharge within the tidal region, D_0 was calibrated in terms of the mixing number α_0. In applying the analytical model to observation, the parameters K, E and α_0 are used as calibration coefficients. Results of the salinity analysis are plotted in Fig. 6. On the whole, it can be said that the analytical salt intrusion model performs well in representing the salinity distribution in all six estuaries despite a few outliers which can be explained.

Some of the deviations in the Bernam and Perak plots may have been caused by timing errors. Data may have been collected slightly earlier or later than HWS (leading to lower values) or LWS (leading to higher values). This was one of the first surveys and the team still had to become experienced in timing the measurements at HWS and LWS. Other deviations can be explained by the physical layout of the estuaries. In Fig. 6(b), the first measurement point at the mouth of Perak estuary during LWS is much lower than the simulated curve. It is believed that this is caused by the sandbar in the middle of the mouth as shown in Fig. 2(b). The existence of the sandbar is linked to dominant ebb and flood channels, which result in lateral variability of the salinity over the width.

For the Selangor plot, the lower values at HWS and LWS are due to the freshwater drainage through sluices shown in Fig. 2(d): it was raining heavily on the day the survey was carried out, and hence drainage water was discharged into the river. This explains why the observed salinity concentrations are lower compared to the simulated values between 11 and 15 km from the mouth. In the Endau plot, it can be seen that there is a deviation from the model, with higher values in the middle reach; the pattern is present in both HWS and LWS. It is probably caused by the tributary at about 8 km from the mouth, as shown in Fig. 2(f). This tributary has less discharge than the Endau River, which causes the water in the tributary to be more saline than in the main estuary. During the tidal cycle, the more saline water that flows in and out of the tributary creates higher salinity concentration near the confluence which propagates upstream. Of all the estuaries studied, the measurements in the Kurau correspond best with the simulated results.

It is also noticeable that the maximum salinity concentration at the mouth varies between estuaries. The Kurau, Bernam, Selangor and Endau estuaries show HWS salinity levels of 30 ppt, whereas the Perak and Muar have only 24 and 27 ppt, respectively. The lower value of the Perak is probably caused by the sand bar extending into the sea. The lower value in the Muar estuary is probably caused by the freshwater discharge from the rivers of Sumatra which affect the salinity near the estuary mouth (the estuary is situated nearest to Sumatra Island).

Figure 6 also shows the total salt intrusion length for each of the estuaries. According to the plots, the salt water intrudes furthest in the Bernam estuary, followed by the Muar, Endau, Perak and Selangor, and is shortest in the Kurau estuary.

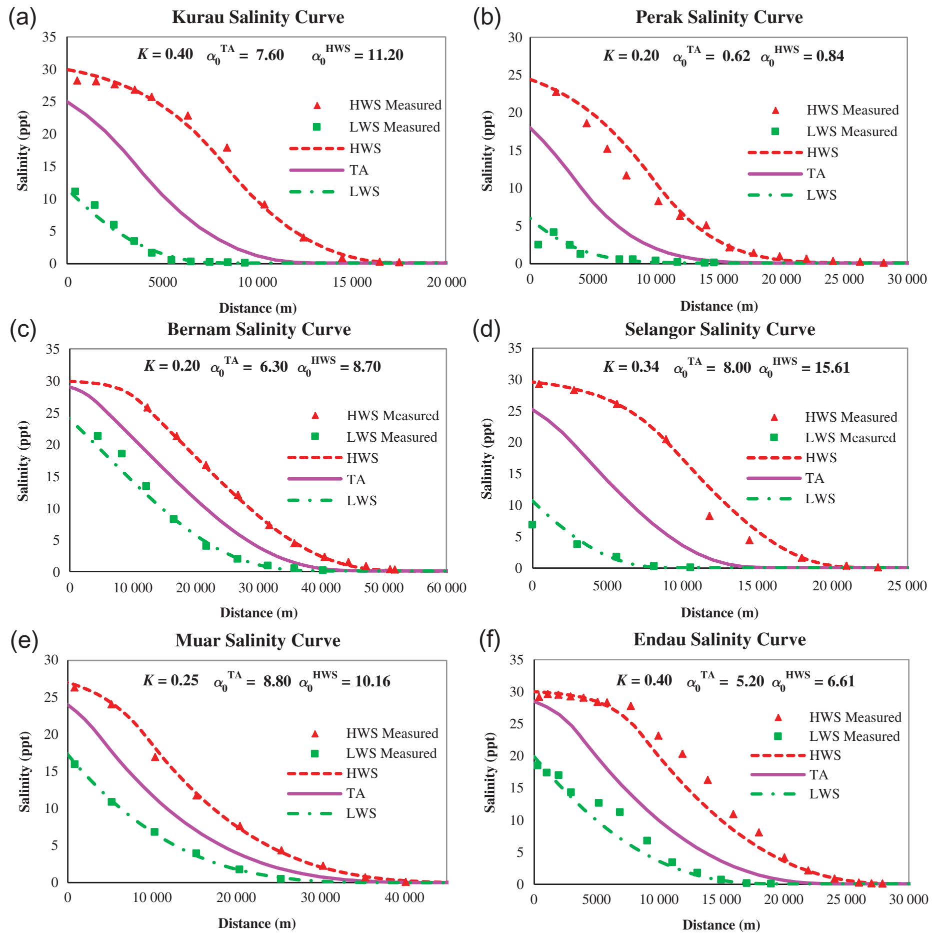

Fig. 6 Measured and simulated longitudinal salinity profiles of the estuaries: (a) Kurau (survey date 28 February 2013); (b) Perak (14 March 2013); (c) Bernam (21 June 2012); (d) Selangor (24 July 2012); (e) Muar (3 August 2012); and (f) Endau (28 March 2013), showing the salinity distribution at HWS (high water slack), TA (tidal average) and LWS (low water slack), as well as the calibrated values of the Van der Burgh's coefficient K and the dispersion–discharge ratio α_0.

5.3 Comparison with the predictive equations

The salt intrusion model was verified by comparing the calibrated K and D_0 values at HWS with the results obtained from the predictive equations (24)–(25). The comparison performed in this study is based on HWS because the data of Savenije (2012), to which the newly surveyed estuaries are compared, were calibrated at HWS. The discharge data, Q_f used to compute D_0 is obtained from the streamflow station nearest to the estuary mouth. This implies that we neglect any inflow from the tributaries between the mouth and the station.

Figure 7(a) demonstrates that the Van der Burgh coefficient K computed from the predictive equation presents a fairly good correlation with the calibrated values except for two estuaries, the Kurau and Endau (outliers). Savenije (2012) concluded that the accuracy of the predictive equation for K is still weak if compared to the calibrated result from measurement, and has to be cautiously applied. Using the predictive equation for K and D_0^{HWS}, the model appears to overestimate the values for the dispersion D_0^{HWS}, mixing number α_0^{HWS} and salt intrusion length L^{HWS}, compared to the calibrated ones as shown in Fig. 7(b)–(d). This is likely due to the underestimation of the freshwater discharge, since it does not account for the intermediate catchments. The most significant deviation is in the Perak estuary. It is known that the nearest available streamflow station is 187 km upstream, and there are several tributaries downstream of it draining to the estuary. The confluences with the tributaries (Bidor, Kinta and Terus rivers) are situated at approximately 65–75 km from the estuary mouth. Because the discharge

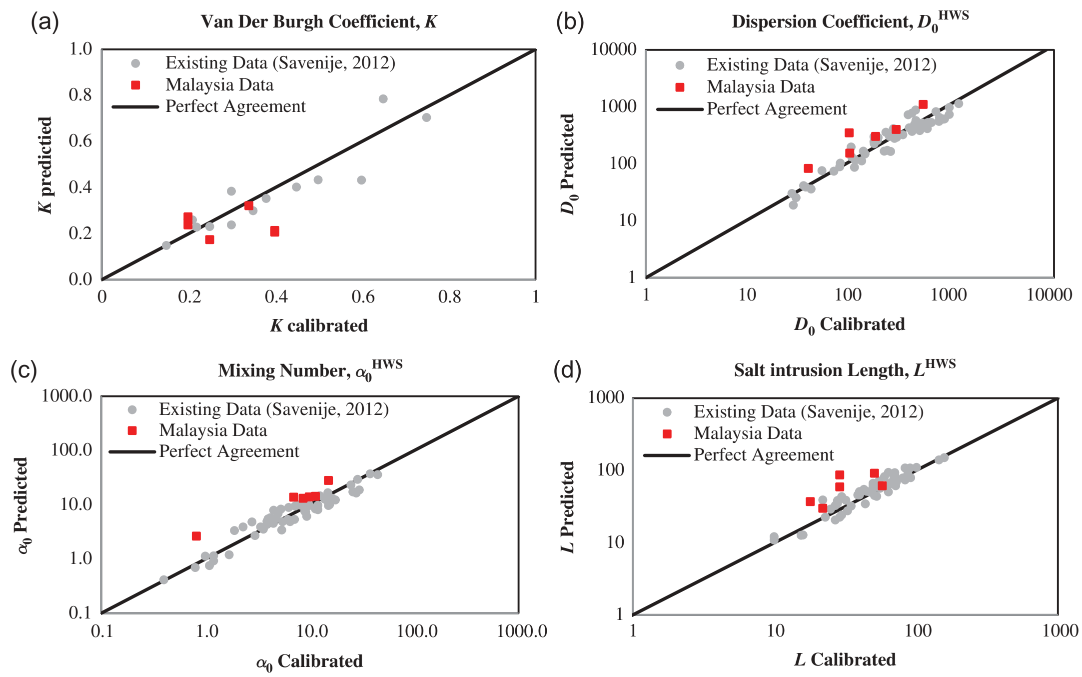

Fig. 7 Comparison between predicted and calibrated results for: (a) Van der Burgh's coefficient K; (b) dispersion coefficient at high water slack D_0^{HWS}; (c) mixing number at high water slack α_0^{HWS}; (d) salt intrusion length at high water slack L^{HWS}. Square markers are the newly surveyed estuaries; round markers are the estuaries reported in Savenije (2012).

from these estuaries is not taken into account, it is reasonable that the calculated salt intrusion length has a higher value than the observed, as the discharge used is too low. Values of the parameters from both approaches are summarized in Table 4.

5.4 Model performance

The performance of the models in simulating and predicting the salt intrusion in estuaries was assessed by evaluating the correlation between the computed and predicted results to the measured data. The model accuracy was defined with two model accuracy statistics: the root-mean-squared error (E_{RMS}) and the Nash-Sutcliffe efficiency (E_{NS}). The equations used to perform the statistical analyses are as shown below:

$$E_{\mathrm{RMS}} = \sqrt{\frac{1}{n}\sum_{i=1}^{n}(P_i - O_i)^2} \quad (28)$$

$$E_{\mathrm{NS}} = 1 - \frac{\sum_{i=1}(P_i - O_i)^2}{\sum_{i=1}(O_i - \bar{O}_i)^2} \quad (28)$$

where P_i is the calculated or predicted value at a certain point or estuaries, O_i is the value observed from measurement, and $\bar{O}_i$ is the average

Table 4 Salinity distribution data showing the salinity at the mouth S_0, Van der Burgh coefficient K, freshwater discharge Q_f, tidal excursion E, plus the dispersion coefficient D_0^{HWS}, mixing number α_0^{HWS} and salt intrusion length L^{HWS}, at high water slack.

Estuary	S_0^{HWS} (ppt)	Q_f (m^3/s)	E (km)	K calib.	K pred.	D_0^{HWS}calib. (m^2/s)	D_0^{HWS}pred. (m^2/s)	α_0^{HWS} calib. (m^{-1})	α_0^{HWS} pred. (m^{-1})	L^{HWS} meas. (km)	L^{HWS} pred. (km)
Kurau	30	28	9.5	0.40	0.21	304	397	11.20	14.17	18	36
Perak	24	132	12.5	0.20	0.24	111	349	0.84	2.64	31	58
Bernam	30	23	14.0	0.20	0.27	203	302	8.70	12.94	58	61
Selangor	30	39	12.7	0.34	0.32	601	1073	15.61	27.88	22	30
Muar	27	11	11.5	0.25	0.17	107	149	10.16	14.12	54	92
Endau	30	6	10.5	0.40	0.21	41	75	6.61	12.21	29	77

Table 5 Results of the model performance in terms of root mean squared error (E_{RMS}) and Nash-Sutcliffe efficiency (E_{NS}).

Salinity model fitting Estuary	E_{RMS}	E_{NS}
Kurau	0.98 ppt	0.99
Perak	1.58 ppt	0.94
Bernam	0.83 ppt	0.99
Selangor	1.71 ppt	0.98
Muar	0.48 ppt	1.00
Endau	1.81ppt	0.97
Predictive models		
Van der Burgh K	0.12	–1.70
Dispersion D_0	210 m^2/s	–0.39
Mixing number α_0	5.8 m^{-1}	–0.86
Intrusion length L^{HWS}	27 km	–2.06

of the observed values. Table 5 displays the outcome of the model accuracy analysis for the salinity models of each estuary and the predictive models.

It is clear in the results that the analytical salt intrusion model has a very good fit for all the estuaries. The E_{RMS} obtained for each estuary is about 1.5 ppt (10% of the average salinity), which is acceptable. The fit of the simulated result with the measurement data is best represented by the NS coefficient, where all the values are near to unity. This means that the analytical salt model is very reliable and efficient in simulating the salinity level in the Malaysian estuaries. However, the performance of the predictive model for the dispersion coefficient is not very satisfactory. The RMS errors are rather large, up to more than 60% of the average value, and for the NS efficiency, the results show negative efficiency which means that the calibrated or observed mean gives better prediction than the model. However, for the Van der Burgh coefficient, the predictive model presents better result with an RMS error of 0.12 (about 40% of the average) while the NS efficiency is still negative.

Although the predictive equations do not perform very well in this study, this appears to be largely due to the uncertainty in the discharge data (underestimated because large parts of the drainage basin are not included in the discharge data used), which can be observed in Figs 8–10. A method to reduce this uncertainty is presented in the next section.

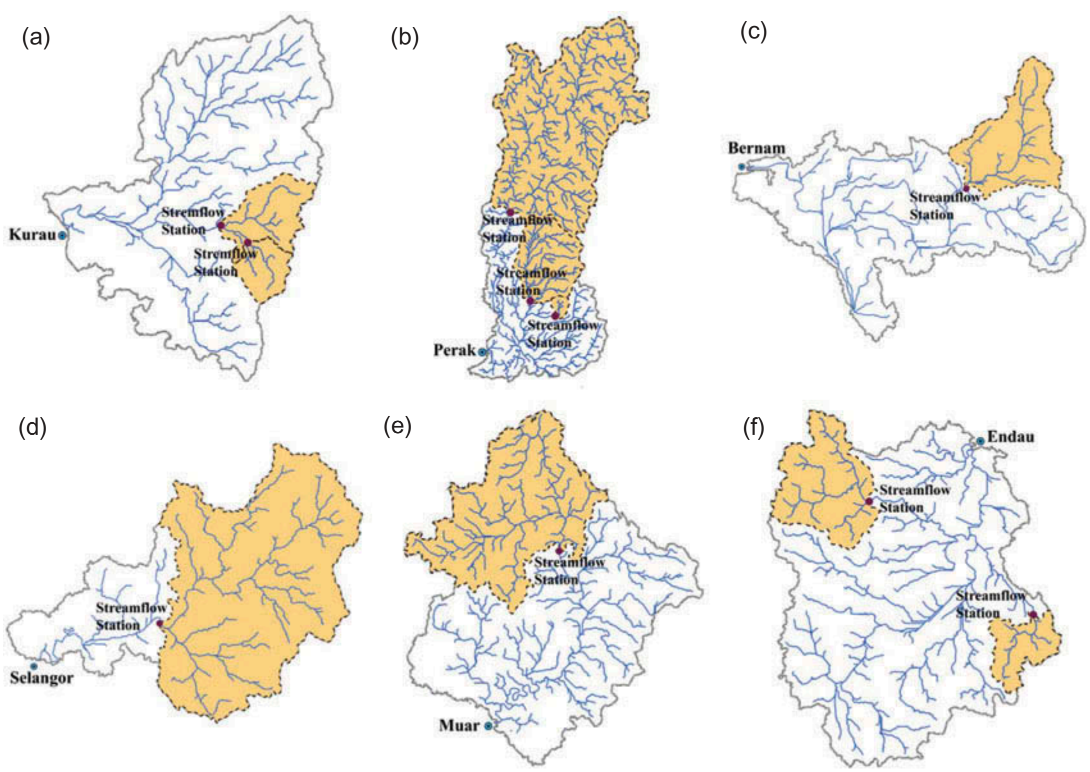

Fig. 8 Maps of the gauged and ungauged watersheds of each estuary (not to scale): (a) Kurau; (b) Perak; (c) Bernam; (d) Selangor; (e) Muar; and (f) Endau estuary, with the gauged area highlighted.

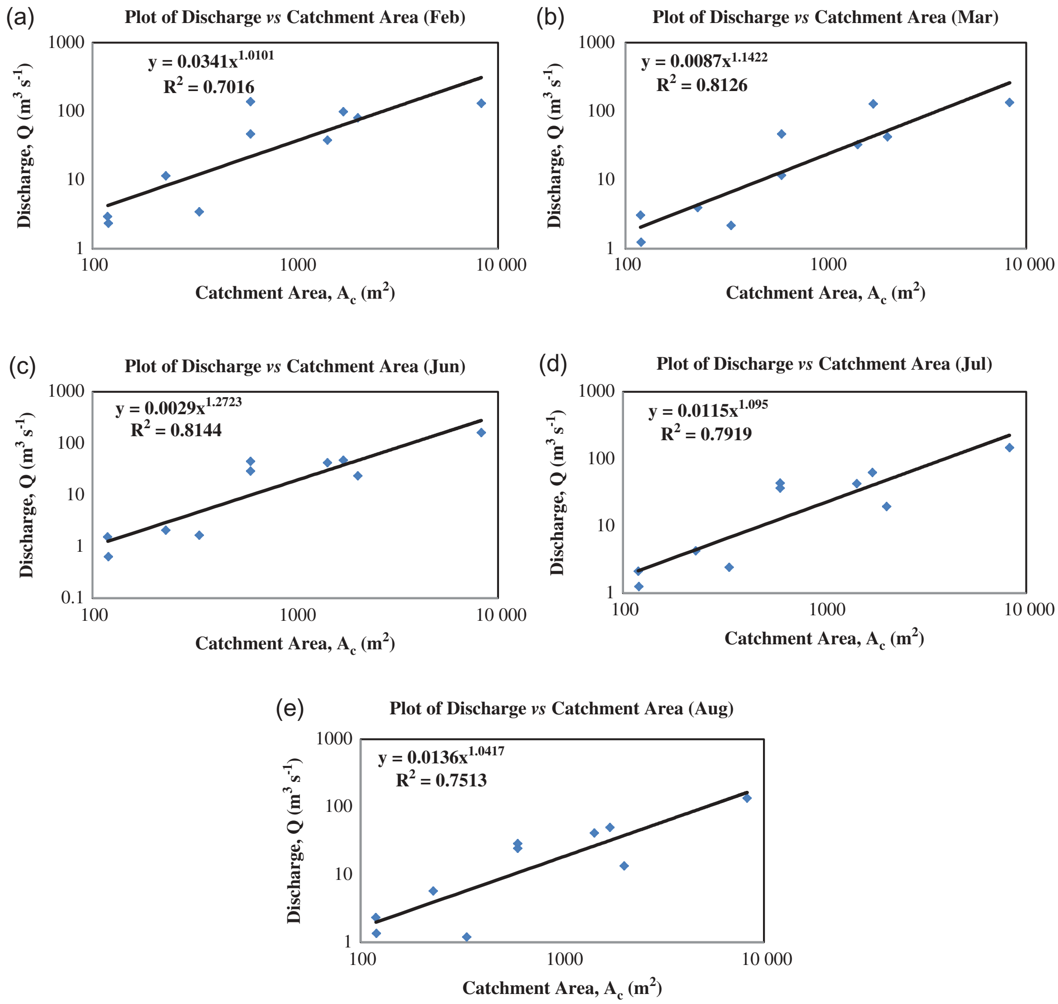

Fig. 9 Power relation between the river discharge and the drainage area during the month of the corresponding salinity measurements: (a) February 2013; (b) March 2013; (c) June 2012; (d) July 2012; and (e) August 2012.

6 CORRECTING FOR THE UNGAUGED WATERSHEDS

6.1 Adjustment of the river discharge

The freshwater discharge uncertainty is considerable in this study due to the unavailability of streamflow data within the tidal region. Because of the influence of the tide, the freshwater discharge becomes very difficult to measure. The best location to collect discharge data is at the point where the tidal influence ends. However, setting up a gauging station at the tidal limit may be inconvenient and costly. Moreover, some estuaries have tributaries that contribute large amounts of freshwater discharge within the tidal region and so are also difficult to define.

In an effort to address this problem, a simple regression between discharge and drainage area has been used to assess the contribution of the ungauged areas to the freshwater discharge into the estuaries, based on the discharge data available in the gauged parts of the catchments. For each month in which salinity was surveyed, the relation between drainage area and discharge was established. This relation was then used to estimate the flow in the remaining catchments.

Figure 8(a)–(f) displays the gauged and ungauged areas for each estuary; most discharge stations only cover a small portion of the entire river basins, while there are also tributaries downstream. Besides the area, one of the more important factors contributing to higher discharge is the topography. Mountainous and hilly catchments such as those of the Kurau and Perak estuary are expected to carry larger flow than the flat lands (e.g. Muar and Endau). Using this information, simple power laws as shown in Fig. 9(a)–(e) were used to relate the observed

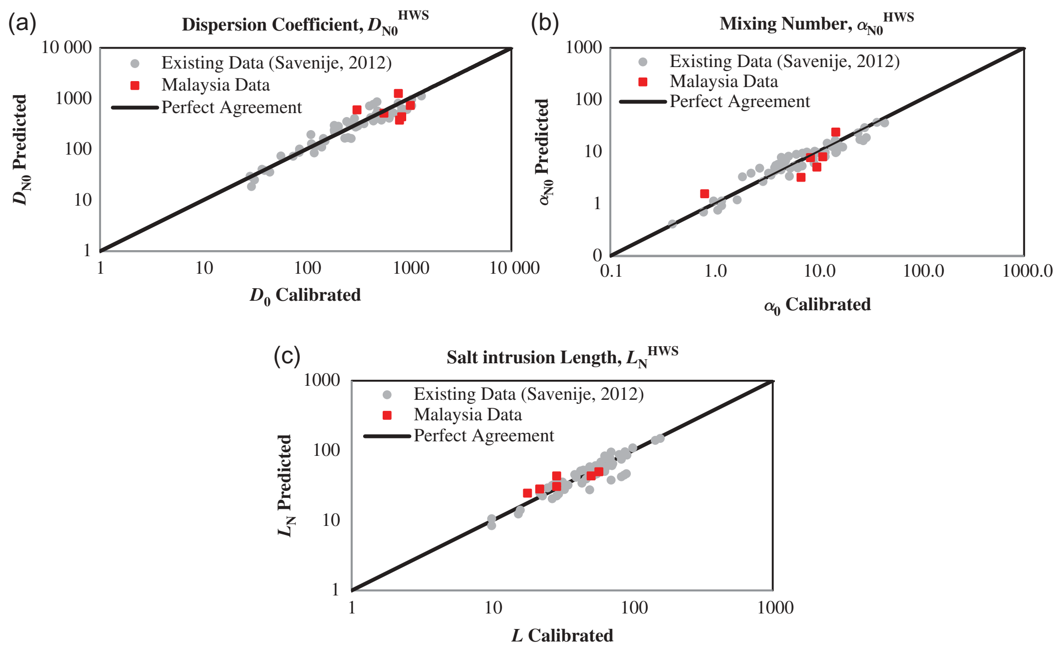

Fig. 10 Comparison between the newly predicted and calibrated results for: (a) dispersion coefficient at high water slack D_{N0}^{HWS}; (b) mixing number at high water slack α_{N0}^{HWS}; (c) salt intrusion length at high water slack L_N^{HWS}. Square markers are the newly surveyed estuaries; round markers are the estuaries reported in Savenije (2012).

discharge to the drainage area. These relationships were subsequently used to compute the discharges for the entire drainage area of the corresponding estuaries.

The adjusted discharges obtained from the power relation were then used in the predictive equation for dispersion to examine how this affects the predicted result. The distributions of the newly calculated parameters are shown in Fig. 10(a)–(c). Table 6 lists the adjusted discharge and predictions, compared to the original ones. The results, in particular the maximum salt intrusion lengths, show clear improvement due to the adjusted discharge values. Since the adjusted freshwater discharge has merely been computed based on the area of the drainage basins, this method tends to over-estimate the discharge from flat land areas such as is the case for the Muar and Endau.

Contrarily, the method still underestimated the amount of discharge for the mountainous and hilly estuaries, especially the Perak. But this is reasonable because the Perak estuary lies in the wettest region in Malaysia. Thus, to balance the intrusion length, larger discharge is required.

6.2 Uncertainty of the predictive models

Besides the uncertainty from the discharge data, there are also uncertainties in the Van der Burgh K and dispersion D_0^{HWS} predictive models. As the models are developed empirically based on datasets from the literature, the reliability of some datasets is

Table 6 Comparison of the predicted parameters with original data for freshwater discharge Q_f, and improved discharge Q_{Nf} – dispersion coefficient D_0^{HWS}, mixing number α_0^{HWS} and salt intrusion length L^{HWS}, at high water slack.

Estuary	Q_f (m^3/s)	Q_{Nf} (m^3/s)	D_0^{HWS} calib. (m^2/s)	D_{N0}^{HWS} calib. (m^2/s)	D_0^{HWS} pred. (m^2/s)	D_{N0}^{HWS} pred. (m^2/s)	α_0^{HWS} calib. (m^{-1})	α_0^{HWS} pred. (m^{-1})	α_{N0}^{HWS} pred. (m^{-1})	L^{HWS} meas. (km)	L^{HWS} pred. (km)	L_N^{HWS} pred. (km)
Kurau	28	92	304	1030	397	719	11.20	14.17	7.81	18	36	23
Perak	132	388	111	326	349	598	0.84	2.64	1.54	31	58	42
Bernam	23	67	203	583	302	512	8.70	12.94	7.64	58	61	49
Selangor	39	53	601	827	1073	1260	15.61	27.88	23.77	22	30	28
Muar	11	87	107	884	149	427	10.16	14.12	4.91	54	92	41
Endau	6	117	41	773	75	327	6.61	12.21	2.80	29	77	25

Table 7 Results of the predictive model performance in term of the root mean-squared error (E_{RMS}) and Nash-Sutcliffe efficiency (E_{NS}) with adjusted discharge values.

Parameter	E_{RMS}	E_{NS}
Dispersion D_0	348 m^2/s	–1.30
Mixing number α_0	4.3 m^{-1}	–0.04
Intrusion length L^{HWS}	8 km	0.72

questionable. In Section 5 it is mentioned that the predictive model for K is rather weak and requires more reliable datasets to strengthen its performance. Better prediction of the K coefficient will improve the efficiency of all the predictive models.

Nevertheless, the overall performance of the predictive model for dispersion improves with the adjusted discharge values. The RMS error and NS efficiency for each parameter are shown in Table 7. Although the new predicted values represent better results, the errors are still large with low NS efficiency. Hence, it is recommended to shift the predictive methods from the HWS to the TA condition as it is believed the model is more stable in the TA situation.

7 CONCLUSIONS

This study has verified that the one-dimensional analytical salt intrusion model is a valid tool for analysing the salt intrusion conditions in six previously unsurveyed estuaries in Malaysia. This model was used for the first time in the Malaysian estuaries and the results are promising. Results from the shape analysis have proved that the geometry of an estuary can be expressed well by branched exponential functions. An excellent fit between the measured salinity and that calculated using the model indicates that all six estuaries can be described by the analytical model. Good correlation between the computed and calibrated Van der Burgh coefficient K shows that the predictive model for K is acceptably efficient for use in these estuaries. However, the over-estimated results for the dispersion D_0, mixing number α_0 and salt intrusion length L suggest that the observed river discharge is probably too low in relation to the actual discharge. This is mainly due to an underestimation of the drainage into the estuaries.

The streamflow stations available are located too far upstream from the salt intrusion region and they only represent a part of the total drainage basin. Using a rather rough area-wise compensation of the river discharge, a much better performance of the predictive equations was obtained. To obtain a more reliable estimate of the discharge into the estuaries, it is recommended to set up a hydrological model for the intermediate catchments making use of the hydrological performance of the nested catchments within these basins.

Though no significant environmental problems were found in these estuaries, this study still provides useful information on their present condition. Moreover, the information obtained is also important in making engineering decisions. The model shows that human interference, such as dredging and freshwater extraction, will increase the salt intrusion length. By utilizing the predictive equations, we can estimate the minimum amount of river discharge needed, and the maximum allowable depth for dredging, to prevent salt water intruding further into the areas concerned. Thus, the simple and effective approach presented in this study can describe the current state of salt intrusion in Malaysian estuaries, and be used for future development. The results also suggests that the Malaysian water authority should consider regulating both water extraction and dredging to avoid severe salt intrusion problems.

Acknowledgements The authors would like to express their gratitude to: Universiti Teknologi Malaysia (UTM) and colleagues Huayang Cai for their invaluable support and assistance in completing the fieldworks in Malaysia; and the Department of Irrigation and Drainage (DID) Malaysia for providing the hydrological data.

REFERENCES

Dronkers, J., 1982. Conditions for gradient-type dispersive transport in one-dimensional, tidally averaged transport models. *Estuarine, Coastal and Shelf Science*, 14 (6), 599–621. doi:10.1016/S0302-3524(82)80002-9.

EPU (Economic Planning Unit Malaysia), 1982. *National Water Resources Study Malaysia Volume 5, Sectoral Report, River Conditions*. National Hydraulic Research Institute of Malaysia (NAHRIM).

Ervine, D.A., Bekic, D., and Glasson, L., 2007. Vulnerability of two estuaries to flooding and salinity intrusion. *Water Science Technology: Water Supply*, 7 (2), 125–136.

Ibrahim, Z.Z., *et al*., 1996. Classification of Malaysian estuaries for development planning. *Aquatic Conservation: Marine Freshwater Ecosystems*, 6, 195–203. doi:10.1002/(SICI)1099-0755(199612)6:4<195::AID-AQC207>3.0.CO;2-9.

Ippen, A.T. and Harleman, D.R.F., 1961. One-dimensional analysis of salinity intrusion in estuaries. *Technical Bulletin no. 5*, Committee on Tidal Hydraulics, Corps of Engineers, US. Army.

Kuijper, K. and van Rijn, L.C., 2011. Analytical and numerical analysis of tides and salinities in estuaries; part II: salinity distributions in prismatic and convergent tidal channels. *Ocean Dynamics*, 61, 1743–1765. doi:10.1007/s10236-011-0454-z.

Nguyen, A.D. and Savenije, H.H.G., 2006. Salt intrusion in multi-channel estuaries: a case study in the Mekong Delta, Vietnam. *Hydrology Earth System Science*, 10, 743–754. doi:10.5194/hess-10-743-2006.

Nguyen, A.D., *et al*., 2008. Using salt intrusion measurements to determine the freshwater discharge distribution over the branches of a multi-channel estuary: the Mekong Delta case. *Estuarine Coastal and Shelf Science*, 77 (3), 433–445. doi:10.1016/j.ecss.2007.10.010.

Nguyen, D.H., Umeyama, M., and Shintani, T., 2012. Importance of geometric characteristics for salinity distribution in convergent estuaries. *Journal of Hydrology*, 448–449, 1–13. doi:10.1016/j.jhydrol.2011.10.044.

Ong, J.E., *et al*., 1991. Characterization of a Malaysian mangrove estuary. *Estuaries*, 14 (1), 38–38. doi:10.2307/1351980.

Risley, J.C., Guertin, D.P., and Fogel, M.M., 1993. Salinity-intrusion forecasting system for gambia river estuary. *Journal of Water Resources Planning and Management*, 119 (3), 339–352. doi:10.1061/(ASCE)0733-9496(1993)119:3(339).

Savenije, H.H.G., 1986. A one-dimensional model for salinity intrusion in alluvial estuaries. *Journal of Hydrology*, 85 (1–2), 87–109. doi:10.1016/0022-1694(86)90078-8.

Savenije, H.H.G., 1988. Influence of rain and evaporation on salt intrusion in estuaries. *Journal of Hydraulic Engineering*, 114, 1509–1524. doi:10.1061/(ASCE)0733-9429(1988)114:12(1509).

Savenije, H.H.G., 1989. Salt intrusion model for high-water slack, low-water slack, mean tide on spreadsheet. *Journal of Hydrology*, 107 (1–4), 9–18. doi:10.1016/0022-1694(89)90046-2.

Savenije, H.H.G., 1993. Predictive model for salt intrusion in estuaries. *Journal of Hydrology*, 148, 203–218. doi:10.1016/0022-1694(93)90260-G.

Savenije, H.H.G., 2005. *Salinity and tides in alluvial estuaries*. Amsterdam: Elsevier.

Savenije, H.H.G., 2012. *Salinity and tides in alluvial estuaries* [online]. Completely revised 2nd ed. Delft University of Technology. Available from: http://hubertsavenije.files.wordpress.com/2012/10/salinityandtides2_02.pdf [Accessed 26 March 2013].

Shaha, D.C. and Cho, Y.K., 2009. Comparison of empirical models with intensively observed data for prediction of salt intrusion in the Sumjin River estuary, Korea. *Hydrology Earth System Science*, 13, 923–933. doi:10.5194/hess-13-923-2009.

Van Breemen, M.T.J., 2008. *Salt intrusion in the Selangor: model study with Delft 3D estuary in Malaysia.* Thesis (Master). University of Twente. Available from: http://essay.utwente.nl/58269/1/scriptie_M_van_Breemen.pdf

Van der Burgh, P., 1972. *Ontwikkeling van een methode voor het voorspellen van zoutverdelingen in estuaria, kanalen en zeeen*. Rijkwaterstaat Rapport, pp. 10–72.

Zhang, E.F., *et al*., 2011. Analytical solution for salt intrusion in the Yangtze Estuary, China. *Estuarine, Coastal and Shelf Science*, 91 (4), 492–501. doi:10.1016/j.ecss.2010.11.008.